

# Leptonic contribution to the effective electromagnetic coupling constant up to three loops

M. Steinhauser

*Max-Planck-Institut für Physik, Werner-Heisenberg-Institut,  
D-80805 Munich, Germany*

## Abstract

In this note the leptonic contribution to the running of the electromagnetic coupling constant is discussed up to the three-loop level. Special emphasize is put on the evaluation of the double-bubble diagrams.

The dominant correction to electroweak observables is provided by the running of the electromagnetic coupling constant from its value at vanishing momentum transfer to high energies. The main part is delivered from the leptonic contribution,  $\Delta\alpha_{\text{lep}}$ , where QED corrections to the photon polarization function,  $\Pi(q^2)$ , have to be considered. The large logarithms of the ratio between the lepton masses,  $M_l$ , and the mass of the  $Z$  boson,  $M_Z$ , is responsible for the size of the corrections. On the other hand the small ratio ensures that it is enough to consider an expansion of  $\Pi(q^2)$  for  $q^2 \gg M_l^2$ . Below in addition to the leading term we will include the first order mass corrections for the one- and two-loop case and demonstrate that the numerical impact is small.

In [1] it is shown that the two-loop term for  $\Delta\alpha_{\text{lep}}(M_Z^2)$  amounts to approximately  $0.78 \times 10^{-4}$  which though is less than 0.3 % of the one-loop value is of the same order of magnitude as the error of the hadronic contribution,  $\Delta\alpha_{\text{had}}^{(5)}$  [1]. Hence, it is interesting to have a look at the three-loop contributions also because there for the first time quadratic logarithms of  $M_l^2/M_Z^2$  appear.

In this note the three-loop diagrams contributing to  $\Pi(q^2)$ , respectively,  $\Delta\alpha_{\text{lep}}$ , are discussed. Thereby only the electron, muon and tau lepton are considered. Virtual quark loops which are present at this order are not taken into account. However, the formulae given below could in principle also be applied to this case.

At one- and two-loop level and for the diagrams relevant for the so-called quenched QED only one mass scale — in the following called  $M_1$  — is involved. Concerning the double-bubble diagrams, however, in general two mass scales,  $M_1$  and  $M_2$ , appear, where

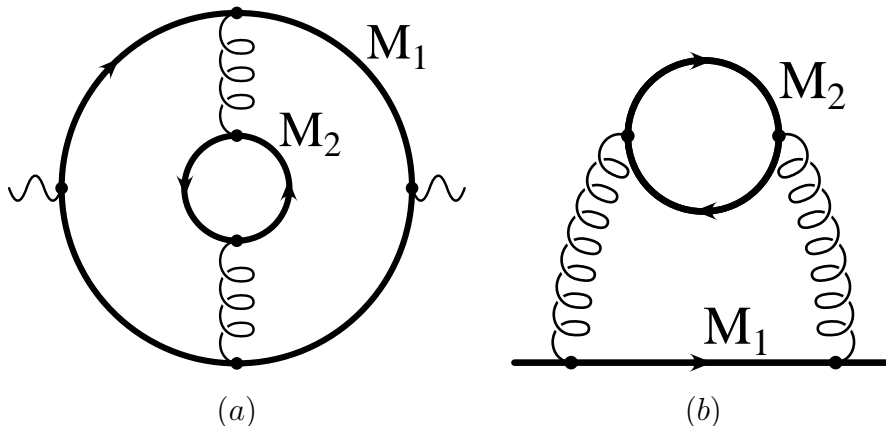


Figure 1: Double-bubble diagram (a) and quark self-energy diagram which is needed for the computation of the mass counterterm (b).

$M_2$  is the mass of the second fermion loop (see Fig. 1(a)). Having in mind the electron, muon and tau lepton three different cases are of practical interest: (i)  $M_1 \gg M_2$ , (ii)  $M_1 = M_2$  and (iii)  $M_1 \ll M_2$ .

The quantity which enters the relation between  $\alpha(0)$  and  $\alpha(M_Z^2)$  is the polarization function,  $\Pi(q^2)$ , evaluated for  $q^2 = M_Z^2$  and normalized in such a way that  $\Pi(0) = 0$ . This means that one has to compute the current correlator both in the limit  $q^2 \gg M_1^2, M_2^2$ , where the masses may be neglected, and for  $q = 0$ . It is convenient to perform the calculation in a first step in a renormalization scheme where the charge and masses are defined in the  $\overline{\text{MS}}$  scheme. The transformation to the on-shell quantities is done afterwards.

The polarization function can be cast into the form

$$\Pi(q^2) = \frac{\alpha}{4\pi} \left[ \Pi^{(0)} + \frac{\alpha}{\pi} \Pi^{(1)} + \left( \frac{\alpha}{\pi} \right)^2 \left( \Pi_A^{(2)} + \Pi_l^{(2)} + \Pi_F^{(2)} + \Pi_h^{(2)} \right) \right], \quad (1)$$

where the double-bubble contributions are given by the last three terms corresponding to the cases (i), (ii) and (iii), respectively.  $\Pi_l^{(2)}$  and  $\Pi_h^{(2)}$  depend on both masses whereas in all other expressions only  $M_1$  appears.  $\Pi^{(0)}$  and  $\Pi^{(1)}$  were already computed in [2]. The results for large external momentum can be found in [3, 4, 5]. Note that in this limit the results for the three cases (i), (ii) and (iii) are identical as mass corrections are neglected. Thus the differences arise from the evaluation of the polarization function for  $q = 0$ . The corresponding results for  $\Pi_A$ ,  $\Pi_l$  and  $\Pi_F$  can be extracted from [6, 4, 5]. To the knowledge of the author the case (iii) was never discussed. Therefore we want to present the result in more detail. For the mass constellation of case (iii) it is not possible to set  $M_1 = 0$  from the very beginning. Rather one has to apply the so-called hard mass procedure [7] in the limit  $M_1^2 \ll M_2^2$ . Furthermore one encounters a two-loop mass counterterm which has to be taken into account (see Fig. 1(b)), which, however, is not yet available in the literature.

Before presenting the results let us in a first step introduce some notation. Throughout the paper on-shell masses are denoted with capital letters;  $\overline{\text{MS}}$  ones with small letters. Bare masses are accompanied with an index “0”. The double-bubble diagrams from case (i) are multiplied with  $n_l$ , the ones from (ii) with  $n_F$  and the ones from (iii) with  $n_h$ .

The relation between the bare and the  $\overline{\text{MS}}$  mass reads [8]:

$$m_1^0 = m_1 \left\{ 1 + \frac{\bar{\alpha}(\mu^2)}{\pi} \left( -\frac{3}{4\varepsilon} \right) + \left( \frac{\bar{\alpha}(\mu^2)}{\pi} \right)^2 \left[ \frac{9}{32\varepsilon^2} - \frac{3}{64\varepsilon} + (n_l + n_F + n_h) \left( -\frac{1}{8\varepsilon^2} + \frac{5}{48\varepsilon} \right) \right] \right\}. \quad (2)$$

Note that the pole parts for the double-bubble diagrams are identical, i.e., they are independent of the mass configuration — a special feature of  $\overline{\text{MS}}$ -like schemes. The transformation to the pole mass is performed with the help of:

$$m_1 = M_1 \left\{ 1 + \frac{\bar{\alpha}(\mu^2)}{\pi} \left( -1 - \frac{3}{4} \ln \frac{\mu^2}{M_1^2} \right) + \left( \frac{\bar{\alpha}(\mu^2)}{\pi} \right)^2 \left[ \frac{7}{128} + \left( -\frac{15}{8} + 3 \ln 2 \right) \zeta(2) - \frac{3}{4} \zeta(3) + \frac{21}{32} \ln \frac{\mu^2}{M_1^2} + \frac{9}{32} \ln^2 \frac{\mu^2}{M_1^2} + n_l \left( \frac{71}{96} + \frac{1}{2} \zeta(2) + \frac{13}{24} \ln \frac{\mu^2}{M_1^2} + \frac{1}{8} \ln^2 \frac{\mu^2}{M_1^2} \right) + n_F \left( \frac{143}{96} - \zeta(2) + \frac{13}{24} \ln \frac{\mu^2}{M_1^2} + \frac{1}{8} \ln^2 \frac{\mu^2}{M_1^2} \right) + n_h \left( -\frac{89}{288} + \frac{13}{24} \ln \frac{\mu^2}{M_2^2} - \frac{1}{8} \ln^2 \frac{\mu^2}{M_2^2} + \frac{1}{4} \ln \frac{\mu^2}{M_1^2} \ln \frac{\mu^2}{M_2^2} \right) \right] \right\}. \quad (3)$$

The terms in the first three lines can be found in [9]. The computation is reduced to the evaluation of two-loop on-shell integrals and can be performed, e.g., with the help of the program package SHELL2 [10]. The terms proportional to  $n_h$  arise from the diagram pictured in Fig. 1(b) which has to be evaluated in the limit  $M_2^2 \gg M_1^2 = p^2$  where  $p$  is the external momentum. The bare diagram was successfully compared with [11]. Using the relation

$$\bar{\alpha}(\mu^2) = \alpha \left[ 1 + \frac{\alpha}{\pi} \frac{1}{3} \left( n_l \ln \frac{\mu^2}{M_2^2} + n_F \ln \frac{\mu^2}{M_1^2} + n_h \ln \frac{\mu^2}{M_2^2} \right) \right], \quad (4)$$

also the coupling can be transformed to the on-shell scheme. Note that the overall factor  $\alpha$  in Eq. (1) is not affected by this change of parameters. The results for the separate contributions to  $\Pi(q^2)$  then read:

$$\Pi^{(0)} = \frac{20}{9} - \frac{4}{3} L_{qM_1} + 8 \frac{M_1^2}{q^2} + \dots, \quad (5)$$

$$\Pi^{(1)} = \frac{5}{6} - 4\zeta(3) - L_{qM_1} - 12 \frac{M_1^2}{q^2} L_{qM_1} + \dots, \quad (6)$$

$$\Pi_A^{(2)} = -\frac{121}{48} + (-5 + 8 \ln 2) \zeta(2) - \frac{99}{16} \zeta(3) + 10\zeta(5) + \frac{1}{8} L_{qM_1} + \dots, \quad (7)$$

$\Delta\alpha_{\text{lep}} \times 10^4$	1-loop	2-loop	3-loop					sum
			quenched	inner lepton			sum	
				$A$	$e$	$\mu$		
$e$	174.34653	0.37983	-0.00014	0.00287	0.00084	0.00025	0.00382	174.73018
$\mu$	91.78419	0.23600	-0.00009	0.00266	0.00084	0.00025	0.00366	92.02385
$\tau$	48.05934	0.16034	-0.00007	0.00214	0.00082	0.00025	0.00314	48.22282
$e + \mu + \tau$	314.19007	0.77617	-0.00030	—	—	—	0.01063	314.97686

Table 1: Contributions to  $\Delta\alpha_{\text{lep}}(M_Z^2) \times 10^4$ .

$$\begin{aligned} \Pi_l^{(2)} = & -\frac{116}{27} + \frac{4}{3}\zeta(2) + \frac{38}{9}\zeta(3) + \frac{14}{9}L_{qM_1} + \left(\frac{5}{18} - \frac{4}{3}\zeta(3)\right)L_{qM_2} \\ & + \frac{1}{6}L_{qM_1}^2 - \frac{1}{3}L_{qM_1}L_{qM_2} + \dots, \end{aligned} \quad (8)$$

$$\Pi_F^{(2)} = -\frac{307}{216} - \frac{8}{3}\zeta(2) + \frac{545}{144}\zeta(3) + \left(\frac{11}{6} - \frac{4}{3}\zeta(3)\right)L_{qM_1} - \frac{1}{6}L_{qM_1}^2 + \dots, \quad (9)$$

$$\Pi_h^{(2)} = -\frac{37}{6} + \frac{38}{9}\zeta(3) + \left(\frac{11}{6} - \frac{4}{3}\zeta(3)\right)L_{qM_2} - \frac{1}{6}L_{qM_2}^2 + \dots, \quad (10)$$

with  $L_{qM_1} = \ln(-q^2/M_1^2)$  and  $L_{qM_2} = \ln(-q^2/M_2^2)$ . The dots represent subleading terms in  $M_l^2/M_Z^2$ . The logarithmic dependence on  $q$  of the double-bubble diagrams coincides, the constant terms are, however, different. It is also worth to mention that  $\Pi_h^{(2)}$  gets independent of  $M_1$ , however, only after the mass is transformed to the on-shell scheme. Note also that  $\Pi_l^{(2)}$  becomes dependent on  $M_2$  after the result is expressed in terms of the on-shell coupling.

For the numerical evaluation of  $\Delta\alpha_{\text{lep}}(M_Z^2)$  the quantity  $-\text{Re}(\Pi(q^2 = M_Z^2))$  has to be considered taking into account the contributions from the electron, muon and tau lepton. Special care has to be taken for those contributions where two masses are involved: In the case of the electron  $\Pi_l^{(2)}$  is not present and  $\Pi_h^{(2)}$  has to be evaluated with  $M_2 = M_\mu$  and  $M_2 = M_\tau$ . For the muon  $\Pi_l^{(2)}$  is used with  $M_2 = M_e$  and  $\Pi_h^{(2)}$  with  $M_2 = M_\tau$ . For the contribution from the tau lepton  $\Pi_l^{(2)}$  has to be evaluated with  $M_2 = M_e$  and  $M_2 = M_\mu$ .

In Tab. 1 the numerical results for  $\Delta\alpha_{\text{lep}}(M_Z^2)$  separated into the contributions from the different lepton species and number of loops are listed. It can be seen that at three-loop order for each lepton the sum of the double-bubble diagrams is larger by a factor of 30 to 40 as compared to the quenched part. The total contribution of  $\mathcal{O}(\alpha^3)$  amounts to  $\approx 1.4\%$  of the  $\mathcal{O}(\alpha^2)$  result and is thus roughly an order of magnitude larger than expected using the naive estimation  $\alpha/\pi \approx 2 \times 10^{-3}$ . This can be traced back to the squared logarithms which are actually only present in  $\Pi_l^{(2)}$ ,  $\Pi_F^{(2)}$  and  $\Pi_h^{(2)}$ . It is also remarkable that the contributions to the double-bubble diagrams are essentially dominated by the mass of the inner lepton which can be understood by a closer look to Eqs. (8)–(10).

A comment concerning the mass corrections  $M_l^2/M_Z^2$  is in order. Obviously the most important contribution comes from the  $\tau$  lepton. It amounts at one-loop level to approxi-

mately  $-2 \times 10^{-6}$  which is of the same order of magnitude as the one from the three-loop diagrams. The quadratic mass corrections of order  $\alpha^2$  are already two orders of magnitude smaller. Therefore we neglect the mass corrections at the three-loop level. In principle also terms of the form  $M_1^2/M_2^2$  are present in the correlator  $\Pi_h^{(2)}$ . However, they are also small and will be neglected.

To summarize, the leptonic contribution to the effective electromagnetic coupling constant is computed up to  $\mathcal{O}(\alpha^3)$ . At three-loop level it turns out that the double-bubble diagrams are most important as quadratic logarithms of the ratio  $M_l^2/M_Z^2$  appear. The total contribution to  $\Delta\alpha_{\text{lep}}(M_Z^2)$  amounts to  $10^{-6}$ .

### Acknowledgments

I would like to thank J.H. Kühn for inspiring and valuable discussions.

## References

- [1] J.H. Kühn and M. Steinhauser, Report Nos. TTP98-05, MPI-PhT/98-12 and hep-ph/9802241.
- [2] G. Källén and A. Sabry, *K. Dan. Vidensk. Selsk. Mat.-Fys. Medd.* **29** (1955) No. 17.
- [3] S.G. Gorishny, A.L. Kataev and S.A. Larin, *Phys. Lett.* **B 259** (1991) 144; L.R. Surguladze and M.A. Samuel, *Phys. Rev. Lett.* **66** (1991) 560; (E) *ibid.*, 2416; K.G. Chetyrkin, *Phys. Lett.* **B 391** (1997) 402.
- [4] P.A. Baikov and D.J. Broadhurst, Presented at *4th International Workshop on Software Engineering and Artificial Intelligence for High Energy and Nuclear Physics (AIHENP95)*, Pisa, Italy, 3-8 April 1995. Published in Pisa AIHENP (1995) 167.
- [5] K.G. Chetyrkin, J.H. Kühn and M. Steinhauser, *Nucl. Phys.* **B 482** (1996) 213.
- [6] D.J. Broadhurst, A.L. Kataev and O.V. Tarasov, *Phys. Lett.* **B 298** (1993) 445.
- [7] For a review see e.g.: V.A. Smirnov, *Mod. Phys. Lett.* **A 10** (1995) 1485.
- [8] R. Tarrach, *Nucl. Phys.* **B 183** (1981) 384.
- [9] N. Gray, D.J. Broadhurst, W. Grafe, and K. Schilcher, *Z. Phys.* **C 48** (1990) 673.
- [10] J. Fleischer and O.V. Tarasov, *Comput. Phys. Commun.* **71** (1992) 193.
- [11] L.V. Avdeev and M.Yu. Kalmykov, *Nucl. Phys.* **B 502** (1997) 419.